Molecular networks linked by Moesin drive remodeling of the cell cortex during mitosis

Chantal Roubinet,[1,4,5] Barbara Decelle,[1] Gaëtan Chicanne,[6,7,8] Jonas F. Dorn,[2] Bernard Payrastre,[6,7,8] François Payre,[4,5] and Sébastien Carreno[1,3]

[1]Cell Biology of Mitosis laboratory and [2]Mitotic Mechanisms and Chromosome Dynamics laboratory, Institute for Research and Immunology and Cancer, and [3]Département de Pathologie et de Biologie Cellulaire, Université de Montréal, Montréal, Québec H3C 3J7, Canada
[4]Centre de Biologie du Développement, [5]Centre National de la Recherche Scientifique Unité Mixte de Recherché 5547, [6]Institut National de la Santé et de la Recherche Médicale U1048, [7]Institut des maladies métaboliques et cardiovasculaires, and [8]Laboratoire d'Hématologie, Centre Hospitalier Universitaire de Toulouse, Université de Toulouse, Université Paul Sabatier, F-31062 Toulouse, Cedex 09, France

The cortical mechanisms that drive the series of mitotic cell shape transformations remain elusive. In this paper, we identify two novel networks that collectively control the dynamic reorganization of the mitotic cortex. We demonstrate that Moesin, an actin/membrane linker, integrates these two networks to synergize the cortical forces that drive mitotic cell shape transformations. We find that the Pp1-87B phosphatase restricts high Moesin activity to early mitosis and down-regulates Moesin at the polar cortex, after anaphase onset. Overactivation of Moesin at the polar cortex impairs cell elongation and thus cytokinesis, whereas a transient recruitment of Moesin is required to retract polar blebs that allow cortical relaxation and dissipation of intracellular pressure. This fine balance of Moesin activity is further adjusted by Skittles and Pten, two enzymes that locally produce phosphoinositol 4,5-bisphosphate and thereby, regulate Moesin cortical association. These complementary pathways provide a spatiotemporal framework to explain how the cell cortex is remodeled throughout cell division.

Introduction

A universal feature of animal cells undergoing mitosis is the series of transformations in their shape necessary to generate two identical daughter cells. Mitotic cell shape remodeling relies on a precise coupling of cortical actomyosin forces with the plasma membrane. At mitosis entry, increased hydrostatic pressure and isotropic cortical contractility drive the characteristic rounding of prometaphase cells (Matzke et al., 2001; Maddox and Burridge, 2003; Carreno et al., 2008; Kunda et al., 2008; Stewart et al., 2011). Subsequently, asymmetry in cortical tensions leads to polar relaxation and equatorial contraction, which contribute to anaphase cell elongation and to cytokinesis (Hickson et al., 2006; Surcel et al., 2010; Sedzinski et al., 2011). Although mitotic stages were originally described more than one century ago (Flemming, 1882), the molecular networks that modify the cortex to drive transformations in the shape of dividing cells remain to be identified.

We and others have shown that Moesin (Moe) plays essential roles in the regulation of cell shape during mitosis in *Drosophila melanogaster* (Carreno et al., 2008; Kunda et al., 2008). Moe is the sole *Drosophila* member of the ERM (Ezrin, Radixin, and Moesin) family of cytoskeletal regulators, which allow, in a signal-dependent manner, bridging of the actin cytoskeleton to the plasma membrane (Fehon et al., 2010). A flexible α-helical linker separates an N-terminal (FERM [4.1 and ERM]) domain from a C-terminal domain (C-ERMAD), which interact with the plasma membrane and with F-actin, respectively. ERM proteins are regulated by a conformational change: in their dormant cytoplasmic state, interaction between the FERM and the C-ERMAD domains masks the two binding surfaces. In response to various signals, ERM proteins open and provide a bridge between actin filaments and the plasma membrane. Activation of ERM proteins involves both the binding of the FERM domain to phosphoinositol 4,5-bisphosphate $(PI(4,5)P_2)$ and the phosphorylation of a conserved threonine residue (T559 in *Drosophila* Moe) located in the C-ERMAD moiety. Although phosphorylation is a hallmark of ERM activation,

Correspondence to Sébastien Carreno: sebastien.carreno@umontreal.ca

Abbreviations used in this paper: CH, calponin homology; dsRNA, double-strand RNA; mRFP, monomeric RFP; PH, pleckstrin homology; $PI(4,5)P_2$, phosphoinositol 4,5-bisphosphate; RC, rapamycin construct; sqh, spaghetti squash; UTR, untranslated region.

The Rockefeller University Press $30.00
J. Cell Biol. Vol. 195 No. 1 99–112
www.jcb.org/cgi/doi/10.1083/jcb.201106048

JCB **99**

THE JOURNAL OF CELL BIOLOGY

interaction with PI(4,5)P$_2$ has emerged as playing important roles in their regulation (Coscoy et al., 2002; Hao et al., 2009; Roch et al., 2010). Current models state that PI(4,5)P$_2$ favors conformational opening and that phosphorylation further stabilizes this open active form at the cell cortex (Fehon et al., 2010).

ERM function and proper regulation is required during cell division in both flies (Carreno et al., 2008; Kunda et al., 2008; Cheng et al., 2011) and mammals (Luxenburg et al., 2011). In *Drosophila*, depletion of Moe or Slik, the kinase necessary to phosphorylate Moe on T559, leads to similar mitotic defects: mutant cells are unable to round at mitosis entry, and their cortex is continuously deformed throughout cell division. Importantly, these cortical defects impinge on additional aspects of mitosis, including spindle morphogenesis and positioning, as well as chromosome segregation (Carreno et al., 2008; Kunda et al., 2008). Therefore, unraveling ERM function and regulation at the cortex represents a key step to better understanding how cell shape transformations are coordinated during division.

Using functional approaches and high-resolution live imaging in *Drosophila* cultured cells, we show here that the regulated activity of Moe orchestrates changes in tension applied at the cortex and thereby, controls cell shape transformations at the successive steps of cell division. Through systematic screenings of candidate regulators, we identify two networks that collectively provide a spatiotemporal control of Moe activity. The first one relies on Pp1-87B, a phosphatase that counteracts activity of the Slik kinase to restrict high Moe function to early mitosis. Then, the PI(4)P 5-kinase Skittles and PI(3,4,5)P$_3$ phosphatase Pten further refine the pattern of activated Moe through the local production of PI(4,5)P$_2$, which is required for both Moe cortical recruitment and phosphorylation. Integration of these two regulatory networks provides a cell cycle–regulated burst of isotropic Moe activation at the cortex, which is required for cell rounding at G2/M transition. Subsequently, the concomitant equatorial enrichment and polar diminution of Moe activity after the anaphase onset synchronizes equatorial contractions with polar relaxation to allow cell elongation and cytokinesis.

Results

Control of Moe activation participates in cell elongation and cytokinesis

As deduced from the pattern of phosphorylated Moe (P-Moe) in fixed samples (Carreno et al., 2008), the location of activated Moe parallels the sites of cortical contractions during mitosis. To gain insight into the role and the regulation of Moe activity at the cell cortex throughout the cell cycle, we examined dynamics of a functional GFP-tagged Moe (Roch et al., 2010) stably expressed in *Drosophila* S2 cells. Time-lapse microscopy confirmed that Moe localization is tightly regulated during the cell cycle. Although mostly cytoplasmic in interphase, Moe-GFP was recruited to the cell cortex upon mitosis entry (Fig. 1 A). Then, it was redistributed into the cytoplasm after furrow ingression, before complete abscission. Throughout mitosis, the spatial pattern of Moe association with the cortex directly correlated

with cell morphology. In prophase, metaphase, and early anaphase, when cells are spherical, Moe-GFP was isotropically associated with the cortex. When cells started to elongate in anaphase B, Moe-GFP was progressively lost from the poles and accumulated at the equator (Fig. 1, B and C; and Video 1).

This dynamic Moe localization likely requires precise regulation of its activity. We tested this hypothesis by substituting endogenous Moe with a constitutively active phosphomimetic mutant, Moe-TD-GFP. To this aim, cells stably expressing Moe-TD-GFP were treated by a double-strand RNA (dsRNA) specifically targeting the 3′ untranslated region (UTR) of endogenous Moe RNA. Under these conditions, hereafter referred to as Moe-TD cells, Moe-TD-GFP accumulated abnormally at the cortex in interphase and remained associated with the polar cortex during cell elongation (Fig. 1, D, F, and G). Although Moe depletion triggered a low rate of cytokinesis failure (Carreno et al., 2008), substituting endogenous Moe by Moe-TD-GFP impaired cytokinesis in 50% of the cells (Fig. 1 E). Because in many cell types completion of cytokinesis relies on proper elongation in anaphase B (Rappaport, 1971), we evaluated the geometry of Moe-TD cells when progressing through anaphase. Indeed, most Moe-TD cells displayed defective elongation, a phenotype associated to cytokinesis failure (Fig. 1 E). It has been shown that anaphase cell elongation requires concomitant equatorial actomyosin contractions and polar relaxation (Hickson et al., 2006). Because activated Moe increases cortical rigidity (Kunda et al., 2008), we hypothesized that Moe overactivation at the polar cortex triggers excessive stiffness by increasing F-actin association and, consequently, blocks cell elongation. Consistently, we measured an increase in F-actin associated with the polar cortex versus the equatorial region in Moe-TD cells (Fig. 1 H). These results indicate that reduction of Moe activity at the polar cortex contributes to cell elongation during anaphase B and thus, to cytokinesis.

Moe controls polar relaxation by regulating polar cortical blebbing

To further investigate the role of Moe in anaphase cell elongation, we imaged cortical dynamics in dividing S2 cells. Since pioneering works (Prothero and Spencer, 1968), several studies have shown that short-lived blebs form at each pole during anaphase elongation (Porter et al., 1973; Fishkind et al., 1991; Burton and Taylor, 1997; Boucrot and Kirchhausen, 2007). These polar blebs have been recently shown to be necessary to release the cortical tension and cytoplasmic pressure created by cytokinetic ring furrowing (Sedzinski et al., 2011). High-resolution analyses of living Moe-GFP cells indicated that Moe was not initially associated with the bleb cortex during its expansion and was recruited at the bleb rim just before retraction. In normal conditions, blebs were rapidly retracted, within a couple of minutes (Figs. 2 A and S1 and Video 2), and thus, displayed a small size (Fig. 2 B). The absence of Moe activity leads to abnormally large cytoplasmic bulges deforming the cortex of dividing cells as observed in fixed samples (Carreno et al., 2008), suggesting that it disrupts cortical organization. We thus analyzed Moe-GFP dynamics in living cells during polar blebbing
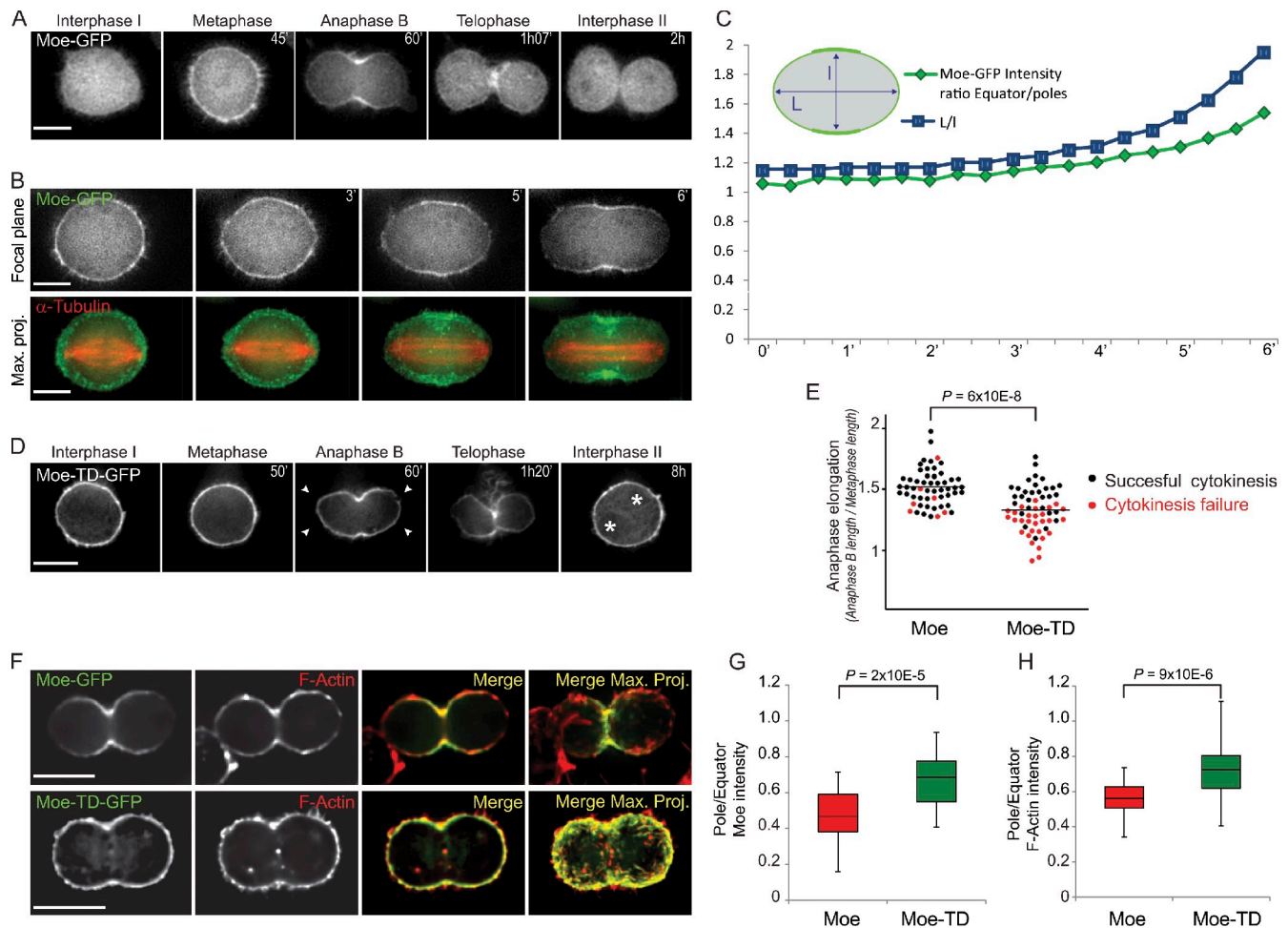
Figure 1. **Control of Moe activation contributes to cell elongation and cytokinesis.** (A) Time lapse of Moe distribution throughout the cell cycle observed in a stable S2 cell line coexpressing Moe-GFP (white) and α-Tubulin-mCherry (not depicted). (B) Dynamics of Moe-GFP during anaphase cell elongation. Top images show a single focal plane of Moe-GFP, and bottom images show maximum projections of Moe-GFP and α-Tubulin-mCherry. (C) Quantification of the equatorial enrichment of Moe-GFP (green) during anaphase elongation (blue) measured as the ratio between cell length along the spindle (L) versus the equator (l). (D) Dynamics of Moe-TD-GFP as observed in living cells upon depletion of endogenous Moe. Moe-TD-GFP remained associated with the polar cortex in anaphase (arrowheads) and caused binucleation (asterisks point to nuclei). (E) Distribution of the maximal elongation of individual Moe-GFP or Moe-TD-GFP cells (cell length in anaphase B/cell length in metaphase). Black dots represent cells that successfully passed through division, and red dots indicate cytokinesis failure. Bars represent mean values for each condition. (F) F-actin distribution in cells expressing Moe-GFP or Moe-GFP-TD upon depletion of endogenous Moe. The right-most images show maximum projection (Max. Proj.). (G and H) Polar enrichment of Moe (G) and F-actin (H) in cells expressing Moe-GFP or Moe-TD-GFP in the absence of endogenous Moe. Boxes show top and bottom quartiles, horizontal lines show median values, and vertical lines show minimal and maximal values. Bars, 10 μm.

and anaphase relaxation in the absence of Slik kinase to preclude Moe activation. Slik depletion decreased the cortical association of Moe-GFP and prevented its recruitment to the bleb cortex (Fig. 2 A and Video 3). Furthermore, similarly to Moe depletion, disrupting Moe activation through Slik knockdown promoted unregulated growth of blebs as well as their delayed retraction, leading to an apparently exaggerated relaxation of the anaphase cortex (Figs. 2 B and S1).

To further explore how Moe controls normal blebbing during polar relaxation in anaphase, we imaged the actomyosin cortex using stable cell lines that expresses the calponin homology (CH) domain of Utrophin fused to GFP to probe actin (Burkel et al., 2007) or the myosin regulatory light chain spaghetti squash (sqh)-GFP to visualize activated myosin (Rogers et al., 2004). In control cells, actin and myosin show similar dynamic association with the bleb cortex. Although they were

not associated with bleb membranes when blebs expand, they were recruited to the bleb cortex when they retract in a manner that parallels the recruitment of Moe (Figs. 2 C and S1 and Video 4). In cells depleted of Moe or Slik, actin and myosin were no longer recruited uniformly to the bleb cortex (Figs. 2 C and S1 and Video 5). Secondary blebs then formed, ultimately leading to multiple blebs on blebs and triggering the abnormal mitotic cytoplasmic bulges observed in fixed samples (Carreno et al., 2008).

Together, these results show that cell division involves a precise regulation of Moe activity to control polar relaxation via mitotic blebbing. Defective Moe cortical recruitment promotes abnormal, unregulated polar blebs and thus, excessive polar relaxation. On the contrary, overactivation of Moe at the polar cortex impairs anaphase relaxation and cell elongation, leading to cytokinesis failure.
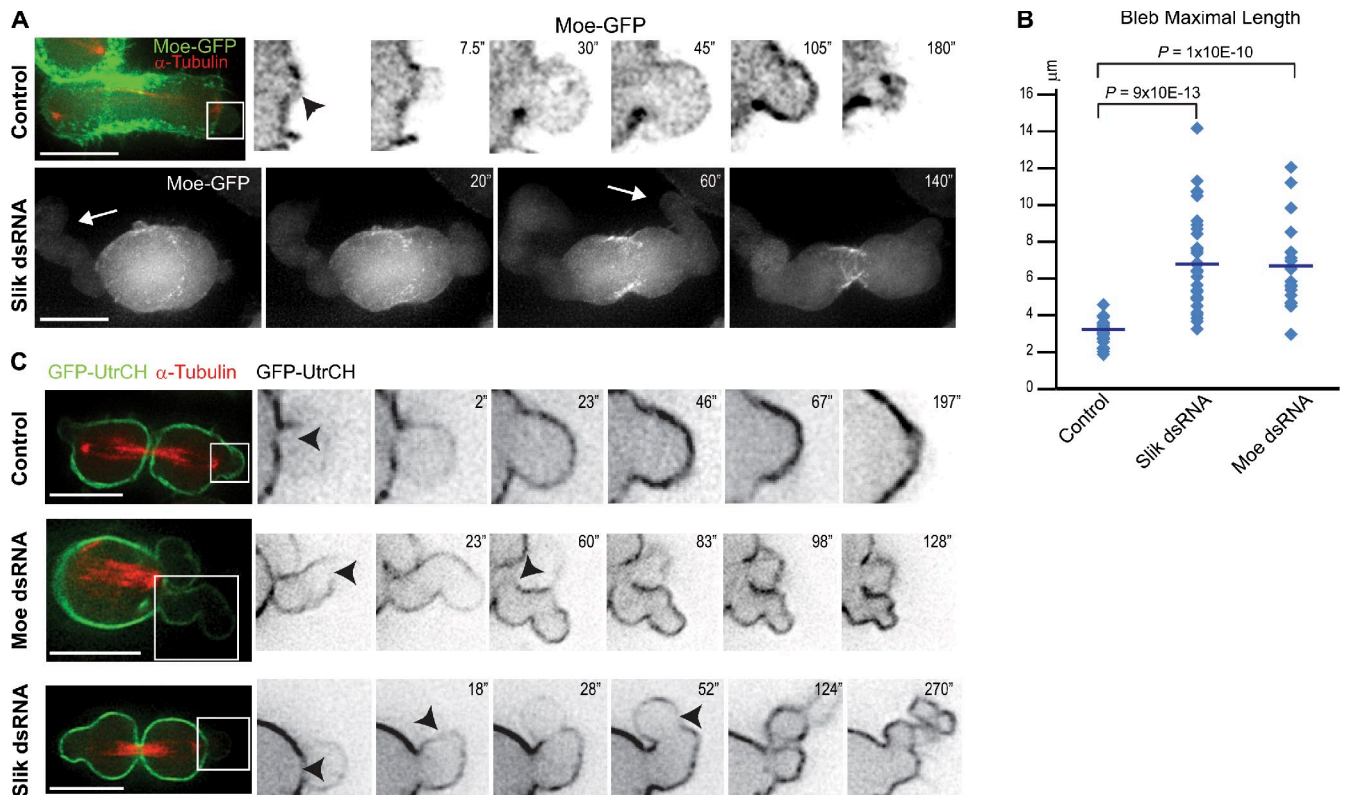
A

Control — Moe-GFP / α-Tubulin — Moe-GFP — 7.5" — 30" — 45" — 105" — 180"

Slik dsRNA — Moe-GFP — 20" — 60" — 140"

B

Bleb Maximal Length

µm

P = 1x10E-10

P = 9x10E-13

16
14
12
10
8
6
4
2
0

Control   Slik dsRNA   Moe dsRNA

C

GFP-UtrCH α-Tubulin   GFP-UtrCH

Control — 2" — 23" — 46" — 67" — 197"

Moe dsRNA — 23" — 60" — 83" — 98" — 128"

Slik dsRNA — 18" — 28" — 52" — 124" — 270"

Figure 2. **Moe controls polar relaxation and retraction of short-lived blebs.** (A) Rapid time-lapse imaging of a cell line coexpressing Moe-GFP and α-Tubulin-mCherry in control condition (top) and after Slik depletion (bottom). The merge image shows maximum projection and close-up single focal planes from the boxed region; Moe-GFP is shown in black. Arrowhead shows an apparent cortical rupture at the site of bleb formation, and arrows point to unregulated blebs. (B) Individual blebs were plotted according to their maximal length in controls cells and after Slik or Moe dsRNA depletion. Bars represent mean values for each condition. (C) Rapid time-lapse imaging of a GFP-Utrophin-CH (GFP-UtrCH; F-actin probe) and α-Tubulin-mCherry cell line in control conditions (top) and after Moe or Slik depletion. Close-ups correspond to the framed region and show the GFP signal in black. Arrowheads show cortical actin rupture and F-actin defective recruitment to the bleb membrane. Bars, 10 µm.

Pp1-87B phosphatase controls Moe inactivation

Having shown that the anisotropic distribution of Moe in anaphase contributes to proper cell division, we then sought to identify regulators of Moe activity. Although Moe activation relies on the activity of Slik kinase (Figs. 3, A and B; and S2 A; Hipfner et al., 2004; Carreno et al., 2008; Kunda et al., 2008), treatment with calyculin A (a PP1 and PP2A phosphatase inhibitor) increased Moe phosphorylation (Fig. 3 A), revealing the existence of a counteracting phosphatase activity.

To identify the phosphatase that inactivates Moe, we individually knocked down each of the *Drosophila* PP1 and PP2A catalytic subunits (Chen et al., 2007) and examined levels of P-Moe by Western blotting. We found that the depletion of Pp1-87B increased Moe phosphorylation (Fig. 3 A). To further identify at which stage of the cell cycle Pp1-87B inactivates Moe, we assessed P-Moe levels by immunofluorescence. We observed that Pp1-87B depletion promoted a threefold increase in Moe phosphorylation at the cortex in interphase (Figs. 3 B and S2 A). Nevertheless, Pp1-87B depletion did not increase P-Moe levels in metaphase, suggesting that Pp1-87B acts to down-regulate Moe at the cortex in interphase. Accordingly, time-lapse analyses showed that after cell division, Moe-GFP was abnormally associated with the cortex of interphase Pp1-87B–depleted cells (Fig. 3 C). In addition, Moe-GFP stayed also aberrantly

associated with the polar cortex during anaphase elongation in Pp1-87B–depleted cells, similar to the distribution of the phosphomimetic Moe-TD mutant form (Fig. 1 D). As observed in Moe-TD cells, Pp1-87B depletion triggered frequent cytokinesis failure (21%, n = 554), further supporting that Moe down-regulation at the polar cortex is required to achieve proper cell division.

To evaluate how Pp1-87B controls Moe activity during the cell cycle, we examined Pp1-87B distribution using a functional GFP fusion (Fig. S2 C). Although mostly cytoplasmic in interphase, GFP–Pp1-87B was redistributed to the mitotic spindle upon mitosis entry (Figs. 3 D and S2 D). Similarly to Pp1-γ, its human orthologue (Trinkle-Mulcahy et al., 2006), GFP–Pp1-87B accumulated on chromosomes, close to the polar cortex in anaphase (Figs. 3 D and S2 D); then, it concentrated to the intercellular bridge where Moe is normally inactivated before abscission (Fig. 1 A). Therefore, dynamics of Pp1-87B distribution inversely correlates with sites of Moe activity. In contrast, Slik associated with the whole-cell cortex in interphase and metaphase and accumulated at the cleavage furrow after the anaphase onset (Fig. 3 D). These data show that a balance of Slik kinase and Pp1-87B phosphatase activities coordinates Moe activation with the cell cycle, restricting high levels of active cortical Moe to early mitosis.
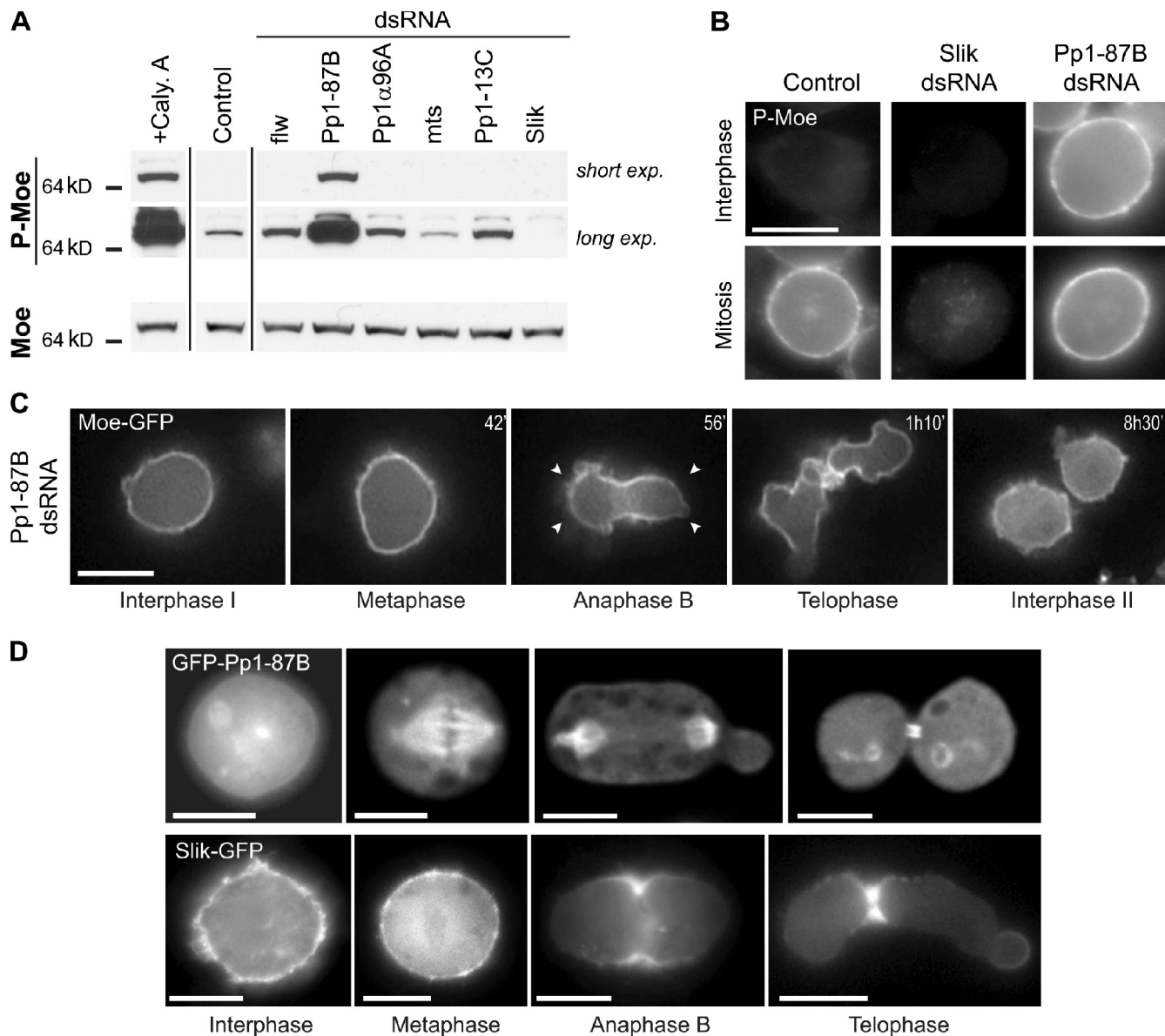
Figure 3. **The Pp1-87B phosphatase down-regulates Moe activation.** (A) Protein extracts from S2 cells treated with Calyculin A (Caly. A) or dsRNAs targeting Slik and the catalytic subunits of each *Drosophila* PP1 and PP2A phosphatases were analyzed by Western blotting using antibodies against Moe (bottom) or specific for T559-phosphorylated Moe (P-Moe; top). The same blot is shown at two different expositions (exp.) for P-Moe. flw, Flapwing; mts, Microtubule star. (B) Immunodetection of P-Moe in control S2 cells or after depletion of Slik or Pp1-87B. (C) Dynamics of Moe-GFP during the cell cycle after depletion of Pp1-87B. Arrowheads show persistence of the association of Moe-GFP with the polar cortex. (D) Distribution of GFP–Pp1-87B (top) and Slik-GFP (bottom). Division stages were identified with α-Tubulin-mCherry (not depicted). Bars, 10 μm.

PI(4,5)P₂ regulates Moe distribution during mitosis

Despite alteration of Moe cortical levels, neither Slik nor Pp1-87B depletion completely abolished the equatorial enrichment of Moe-GFP when cells progress through anaphase (Figs. 2 A and 3 C). Furthermore, the reciprocal phospho mutant forms of Moe, Moe-TD-GFP (Fig. 1 D) and Moe-TA-GFP (Fig. S3), remained enriched at the equatorial cortex in anaphase. These findings suggest that a phosphorylation-independent mechanism regulates the cortical distribution of Moe after the anaphase onset. Binding of the FERM domain to $PI(4,5)P_2$ plays a key role in Moe function in vivo (Roch et al., 2010), opening the possibility that $PI(4,5)P_2$ could contribute to the regulation of Moe activity/distribution during cell division.

As a first test of this hypothesis, we examined the distribution of the Moe FERM domain fused to GFP ($FERM^{Moe}$-GFP) in live cells. Although $FERM^{Moe}$-GFP isotropically associated with the cortex from interphase to metaphase, it was then enriched at the equatorial cortex in anaphase B and telophase (Fig. 4 A). Reciprocally, a full-length Moe mutant (Moe-KN-GFP) unable to bind to $PI(4,5)P_2$ (Roch et al., 2010) was not associated with the cortex throughout mitosis (Fig. 4 A). Therefore, $PI(4,5)P_2$ binding is required for Moe enrichment at the anaphase equator.

We then examined the localization of $PI(4,5)P_2$ in a S2 cell line that stably expresses GFP-Tubby, a specific probe for this phosphoinositide (Szentpetery et al., 2009; Ben El Kadhi et al., 2011). As observed for Moe-GFP (and $FERM^{Moe}$-GFP), GFP-Tubby cleared from polar regions and concentrated at the
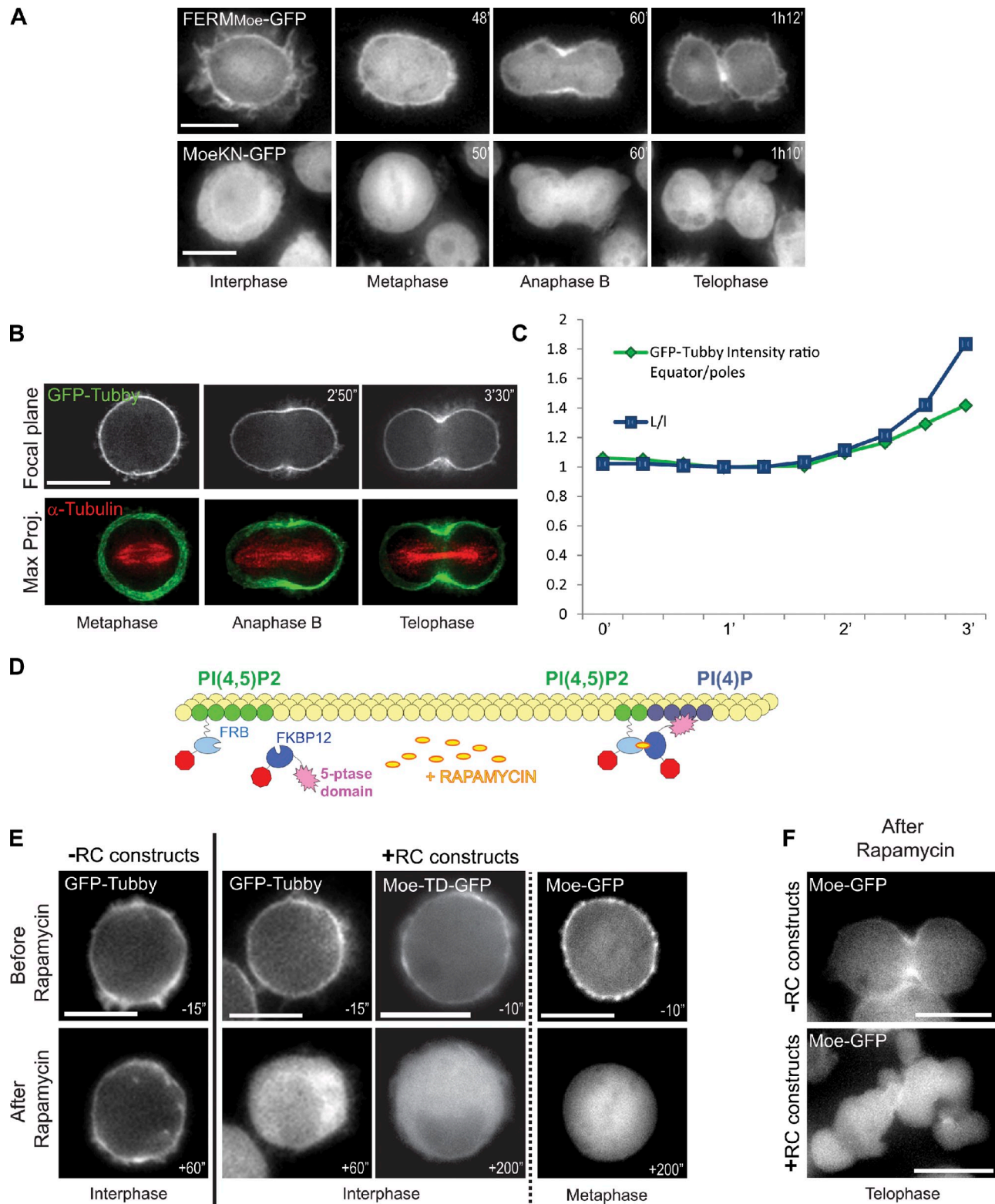
Figure 4. **PI(4,5)P$_2$ regulates Moe distribution during mitosis.** (A) Time-lapse frames of cells stably expressing the N-terminal FERM domain of Moe fused to GFP (top) or a full-length mutant form of Moe (Moe-KN-GFP; bottom) at which point mutations in the FERM domain abolish binding to PI(4,5)P$_2$ (Roch et al., 2010). (B) Dynamics of GFP-Tubby, a PI(4,5)P$_2$ probe in a living S2 cell undergoing mitosis. Max Proj., maximum projection. (C) Quantification of the equatorial enrichment of GFP-Tubby (green) and of anaphase cell elongation (blue). L, length along the spindle; l, length along the equator. (D) Schematic representation of rapamycin-induced dephosphorylation of PI(4,5)P$_2$. Protein domains expressed from RC constructs heterodimerize upon rapamycin addition causing dephosphorylation of PI(4,5)P$_2$ at the plasma membrane (Varnai et al., 2006). (E) Cell lines stably expressing GFP-Tubby, Moe-GFP, or Moe-TD-GFP were transfected (+RC) or not transfected (−RC) by RCs. Living interphase or metaphase cells were imaged just before and after rapamycin addition. (F) Rapamycin-treated Moe-GFP cells in telophase expressing (+RC) or not expressing (−RC) RC constructs. Bars, 10 µm.

equator when cells started to elongate in anaphase (Fig. 4, B and C). These results support the idea that $PI(4,5)P_2$ contributes to the local control of Moe activation during cell division.

To directly test this conclusion, we used a system that rapidly reduces $PI(4,5)P_2$ cortical levels (Varnai et al., 2006), through a rapamycin-inducible recruitment of a type IV phosphoinositide 5-phosphatase domain to the plasma membrane (Fig. 4 D). In this assay, rapamycin induces the heterodimerization between a membrane-targeted FKBP-rapamycin–binding domain fragment of mammalian target of rapamycin and a 5-phosphatase domain fused to FKBP12 (Varnai et al., 2006), individually expressed from two constructs, hereafter referred to as rapamycin constructs (RCs). Although addition of rapamycin to control cells did not modify the localization of GFP-Tubby (Figs. 4 E and S4 A), rapamycin promoted its rapid translocation from the membrane to the cytosol in RC cells (Figs. 4 E and S4 B [for quantification] and Video 6). These results validate the efficiency of the RC system in S2 cells and the specificity of the GFP-Tubby probe for $PI(4,5)P_2$. We then explored whether reduction of $PI(4,5)P_2$ affects the distribution of wild-type or TD Moe-GFP. Moe-TD displayed a strong cortical association in interphase, which was lost after rapamycin treatment in RC cells (Fig. 4 E). Furthermore, when rapamycin was added on RC cells in metaphase, Moe-GFP rapidly delocalized from the cortex to the cytoplasm (Figs. 4 E and S4 C [for quantification] and Video 7). Similarly to Moe dsRNA depletion, this rapamycin-inducible release of Moe from cortical membranes triggered excessive polar relaxation, with unregulated blebbing during cell elongation (Fig. 4 F and Video 8). Together, these results support that $PI(4,5)P_2$ is necessary to ensure mitotic cortical stability, at least in part, through regulation of Moe cortical distribution and activation.

Localized activity of Skittles and Pten controls sites of PI(4,5)P₂ production and of Moe activation

To further investigate how $PI(4,5)P_2$ regulates mitotic cortical stability and Moe activation, we individually depleted each of the *Drosophila* kinases (10), phosphatases (16), and phospholipases (5) predicted to directly or indirectly control $PI(4,5)P_2$ metabolism (Figs. 5 A and S5), and we assessed the consequences of these depletions on the mitotic cortex by time-lapse microscopy. Among the 31 enzymes we have tested, depletion of three proteins induced high cortical defects, including excessive polar relaxation and unregulated blebs during anaphase (Figs. 5 B and S5). Two of them, Skittles and Pten directly produce $PI(4,5)P_2$ by phosphorylating $PI(4)P$ and dephosphorylating $PI(3,4,5)P_3$, respectively. The third enzyme, encoded by CG10260 and predicted to produce $PI(4)P$ from phosphatidylinositol, was required to a lesser extent for mitotic cortical stability (Fig. 5 B). To quantify the respective contribution of these enzymes to $PI(4,5)P_2$ production, we measured cellular phosphoinositides using radiolabeling assays (Payrastre, 2004). $PI(4,5)P_2$ pools were decreased by 15, 31, and 48% after depletion of CG10260, Pten, or Skittles, respectively (Fig. 5 C). Consistently, although the cortical association of GFP-Tubby was only slightly reduced by depletion of CG10260 (not depicted),

the absence of Pten or Skittles further prevented the cortical recruitment of this biosensor, showing that these enzymes generate $PI(4,5)P_2$ at the cortex (Fig. 5 D).

Having shown that Skittles and Pten play major roles in $PI(4,5)P_2$ production in S2 cells, we first examined whether their localization could account for $PI(4,5)P_2$ enrichment at the equator in anaphase. Comparable with $PI(4,5)P_2$ dynamics, Pten-GFP and Skittles-GFP uniformly associated with the cortex in prometaphase. Both enzymes then progressively accumulated at the equator, as cells underwent anaphase elongation (Fig. 6, A and B). Because Pten metabolizes $PI(3,4,5)P_3$, we analyzed the distribution of this $PI(4,5)P_2$ precursor during cell division using the Grp1-pleckstrin homology (PH)-GFP–specific $PI(3,4,5)P_3$ probe (Gray et al., 1999). In control cells, Grp1-PH-GFP was weakly associated with the cortex of mitotic cells, albeit enriched at the cleavage furrow in anaphase (Fig. 6 A). Pten depletion increased the cortical levels of Grp1-PH-GFP, with accumulation at the anaphase equator, where Pten normally localizes. This indicates that Pten locally dephosphorylates $PI(3,4,5)P_3$ to control $PI(4,5)P_2$ cortical levels during mitosis. Accordingly, depletion of Pten provoked the formation of abnormal long-lived polar blebs, a phenotype reminiscent of that seen after rapamycin-induced reduction of $PI(4,5)P_2$. The absence of Skittles further decreased cortical $PI(4,5)P_2$ levels during mitosis, as deduced from its impact on GFP-Tubby distribution (Fig. 6 B). The depletion of Skittles also enhanced unregulated polar blebbing in anaphase (Fig. 6 B), mimicking the defects observed in cells with reduced $PI(4,5)P_2$ levels by the RC experiment (Fig. 4 F) or those lacking Moe activity (Fig. 2, A and C).

We then tested whether Skittles or Pten was required for Moe phosphorylation during mitosis, using FACS analysis of cells costained for P-Moe and the mitotic marker phospho–histone H3. When compared with control conditions, Pten depletion caused a slight decrease in P-Moe levels (27.7% of mitotic cells negative for P-Moe staining vs. 17% in controls). These defects were enhanced when Skittles was depleted, with 81.7% of mitotic cells displaying reduced levels of Moe phosphorylation (Fig. 6 C).

Accordingly, Skittles depletion impaired the association of Moe-GFP with the mitotic cortex (compare Fig. 6 D and Video 9 with Fig. 1 A). This lack of Moe recruitment at the cortex of polar blebs correlated with defects in actin organization (Fig. 6 E and Video 10) and triggered the "blebs on blebs" phenotype and unregulated bleb growth (5.57 ± 1.58–µm length, $n = 26$ vs. 3.25 ± 0.44–µm length, $n = 40$ in controls; $P = 1.5 \times 10^{-8}$) observed after Moe or Slik depletion (Fig. 2, A and C).

These results show that Skittles and Pten contribute to enrich $PI(4,5)P_2$ at the equator, when dividing cells progress through anaphase. Thus, Skittles and Pten spatially mediate Moe cortical activation to promote efficient bleb dynamics necessary to control anaphase cell elongation.

Discussion

These findings unravel how, by integrating two regulatory networks, Moe activity provides a spatiotemporal framework to control cell shape transformations during division (Fig. 7).
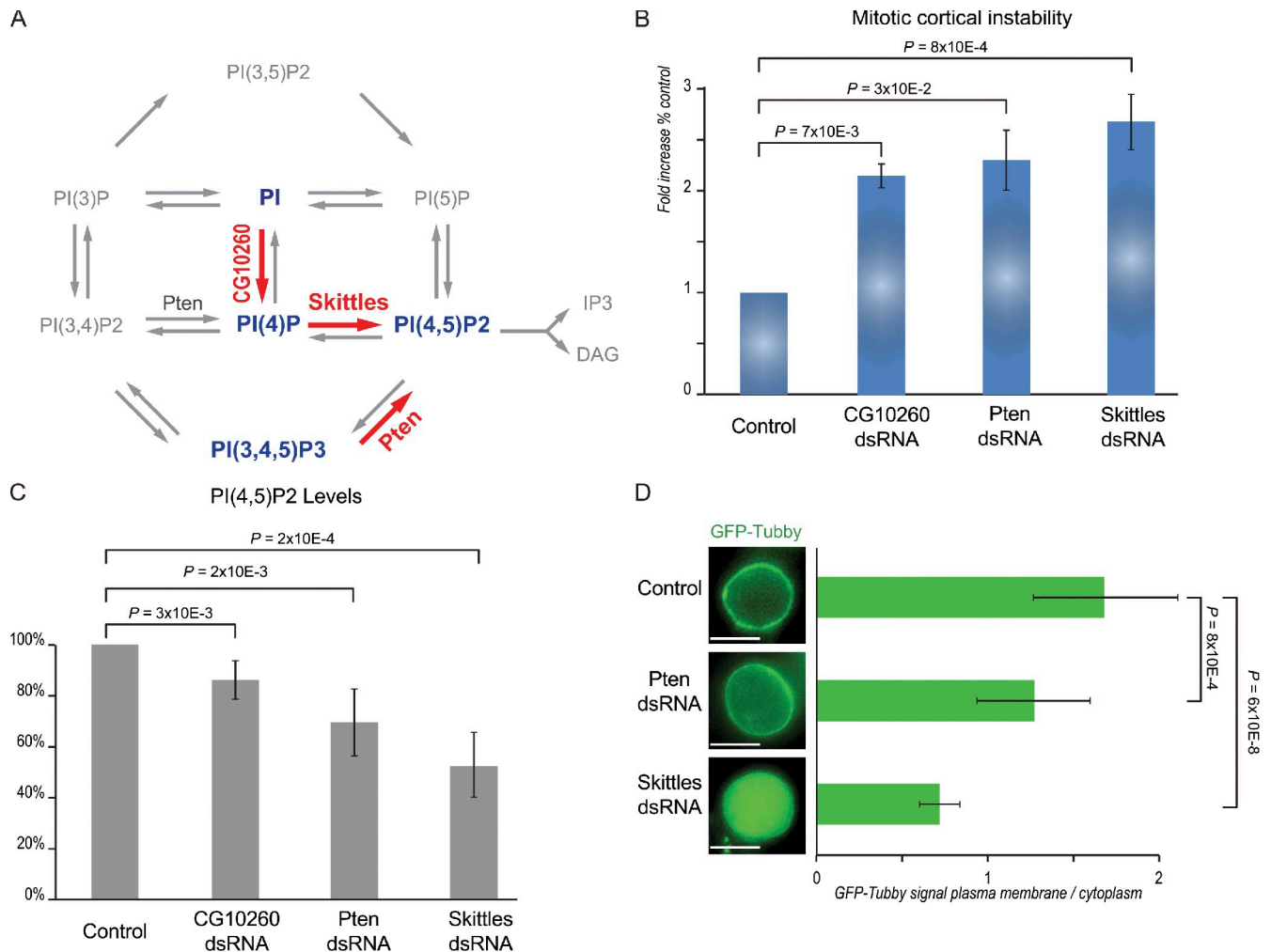
Figure 5. **Depletion of Skittles and Pten destabilizes the mitotic cortex.** (A) Schematic representation of phosphoinositide (PI) pathways. Each of 31 enzymes was individually inactivated by dsRNA, and its influence on cortical stability was analyzed by time-lapse imaging of α-Tubulin-GFP cells undergoing mitosis (n > 100 cells per condition). (B) The graph plots the percentage of cells with mitotic blebbing in control condition and after inhibition of CG10260, Pten, or Skittles. (C) Cellular levels of PI(4,5)P$_2$ in controls and in cells after depletion of CG10260, Pten, or Skittles, as measured by biochemical assays. An arbitrary value of 1 was attributed to levels observed in wild-type cells. (D) Influence of Pten and Skittles on PI(4,5)P$_2$ levels at the cortex of S2 cells. Pictures show GFP-Tubby cells in control conditions and after Pten or Skittles depletion. The graph plots the percentage of cells showing membrane association of GFP-Tubby in each condition. Error bars represent SD. Bars, 10 µm.

We find that the increase in cortical rigidity that drives cell shape remodeling at the interphase/mitosis transition involves a Pp1-87B/Slik molecular switch that timely regulates Moe phosphorylation. We further identify PI(4,5)P$_2$ as a spatial cue that controls Moe distribution at the cortex. This latter aspect coordinates the spatial balance in cortical stiffness/contractility that is required for anaphase cell elongation and cytokinesis. We propose that the concerted action of these two regulatory networks ensures the proper series of mitotic cell shape transformations required for the fidelity of cell division (Fig. 7).

A Pp1-87B/Slik molecular switch controls temporal activation of Moe

A global increase in cortical actomyosin forces generate cell rounding at mitosis entry (Maddox and Burridge, 2003; Stewart et al., 2011). These forces are transmitted to the plasma membrane through the activation of ERM proteins (Carreno et al., 2008;

Kunda et al., 2008; Luxenburg et al., 2011). At mitosis exit, both cortical contractions and ERM activity must be down-regulated to allow cells to go back to their interphase shape. In *Drosophila* cells, the Slik kinase was shown to activate Moe at mitosis entry (Carreno et al., 2008; Kunda et al., 2008). Here, we identify the Pp1-87B phosphatase as essential for Moe inactivation after cytokinesis and in interphase.

Although Slik homogenously associates with the cell cortex in both interphase and early mitosis, Pp1-87B is cytoplasmic in interphase and relocalizes to the spindle in pro/metaphase (Fig. 7 B). An attractive model would be that together with a "constitutive" cortical association of the Slik activator in interphase and pro/metaphase, intracellular redistribution of the Pp1-87B inhibitor represents an efficient way to restrict high levels of Moe phosphorylation to mitosis entry. During anaphase, Pp1-87B concentrates near the chromosomes migrating toward the polar cortex, whereas Slik accumulates at the cleavage furrow. In this model, redistribution of both Pp1-87B
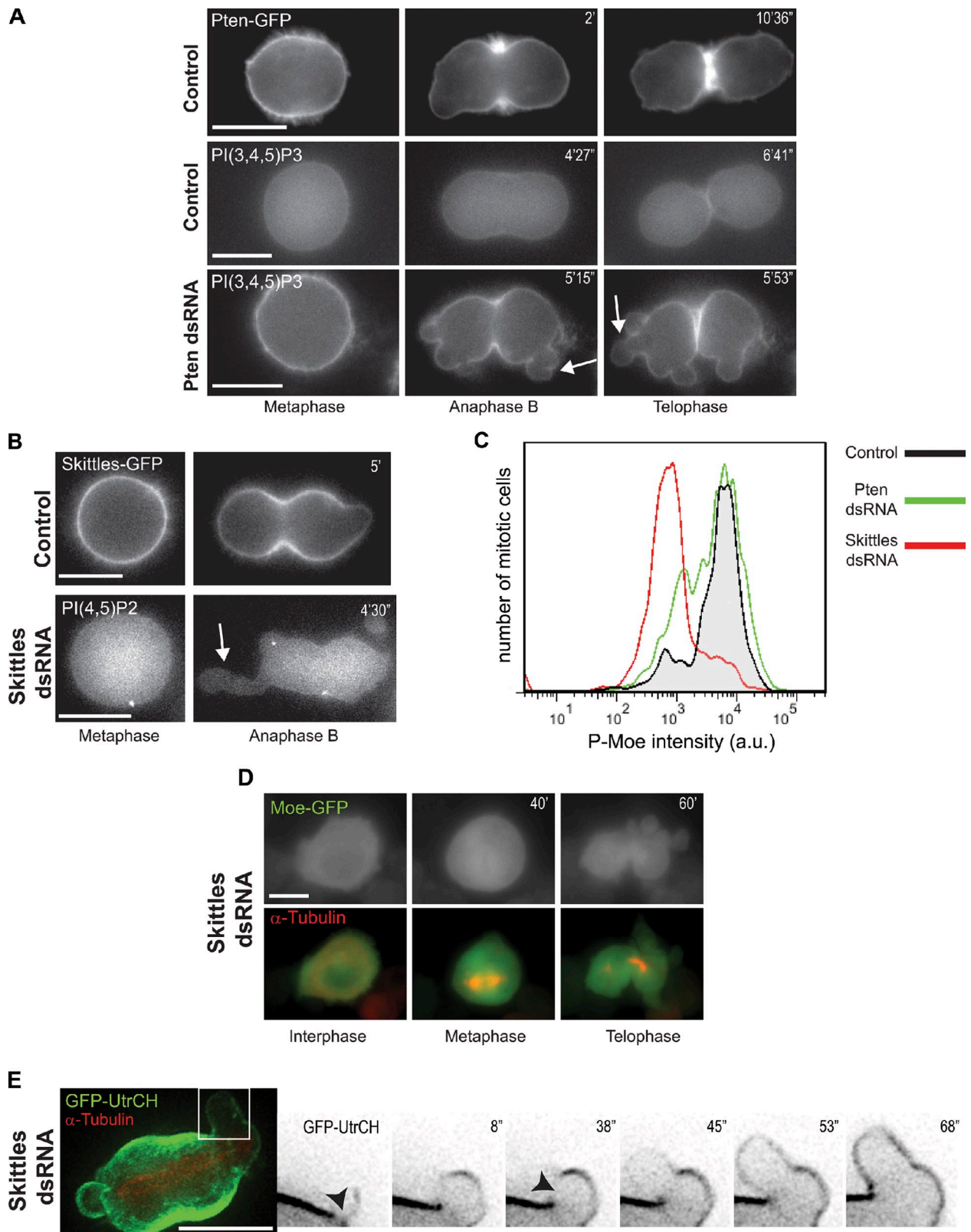
Figure 6. **Localized activity of Skittles and Pten controls sites of PI(4,5)P$_2$ production and Moe activation.** (A) Dynamic of Pten-GFP distribution during mitosis (top). A stable cell line that expresses Grp1-PH-GFP was used to probe PI(3,4,5)P$_3$ distribution during mitosis in control conditions or after Pten depletion. (B, top) Time-lapse frames of a Skittles-GFP cell progressing through mitosis. Bottom images show a living cell stably expressing GFP-Tubby after Skittles depletion. (C) FACS analysis showing the distribution P-Moe intensity in mitosis (assessed by histone H3 phosphorylation) of control and Pten- or Skittles-depleted cells. a.u., arbitrary unit. (D) Distribution of Moe-GFP after Skittles depletion. (E) Rapid time-lapse imaging of a GFP-Utrophin-CH (GFP-UtrCH) and α-Tubulin-mCherry after depletion of Skittles showing maximum projection. Close-ups (focal planes) correspond to the framed region and show GFP signal in black. Arrowheads show cortical rupture and defects of F-actin recruitment at the bleb rim; arrows show unregulated mitotic blebs. Bars, 10 µm.
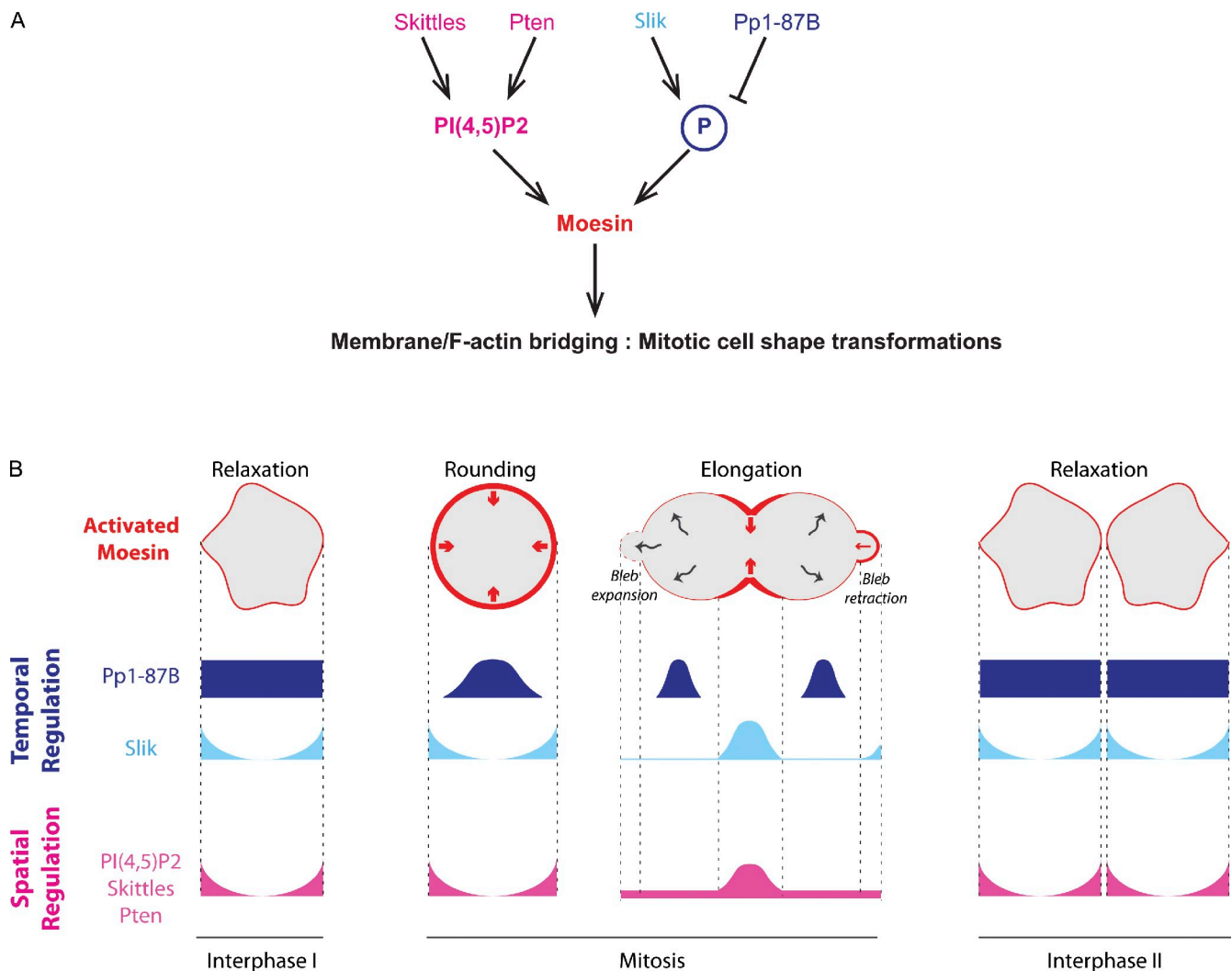
Figure 7. **Model of the spatiotemporal regulation of Moe activity throughout the successive steps of the cell cycle.** The cell cortex that comprises the plasma membrane and the underlying cytoskeleton works as a single functional unit to control cell morphology. (A) Two pathways temporally and spatially control coupling of actin filaments to the plasma membrane through the regulation of Moe activity. (B) Redistribution of the Pp1-87B phosphatase at mitosis entry is likely to promote a burst of Slik-dependent phosphorylation of Moe at early mitotic stages and then ensures Moe down-regulation at the end of division and in interphase. The localized enrichment of Skittles and Pten acts to increase PI(4,5)P_2 levels at the anaphase equator, further promoting Moe recruitment at the equator and release at the polar cortex to allow cell elongation. The same players are involved in the transient recruitment and activation of Moe at the cortex of polar blebs, which is important for their efficient retraction. P, phosphorylation.

and Slik after the anaphase onset contributes to enrich Moe at the equator and to decrease it at poles. Finally, relocalization of Pp1-87B in the cytoplasm after cytokinesis would contribute to relax the cortex for the next interphase by maintaining low Moe activity (Kunda et al., 2008; Théry and Bornens, 2008). A growing number of evidence supports that Pp1 phosphatases play important roles in the temporal control of cell division (De Wulf et al., 2009). Pp1-87B being required for mitotic spindle morphogenesis (Axton et al., 1990; Chen et al., 2007), this phosphatase could contribute to synchronize cell shape control operated through Moe regulation to chromosome segregation. Although additional investigations will be required to unravel how the activity and distribution of Pp1-87B and Slik are regulated, these results indicate that the Slik/Pp1-87B switch represents an important control of Moe activity during the cell cycle.

PI(4,5)P_2 controls stability of the mitotic cortex and spatial activation of Moe

Our results show that local levels of PI(4,5)P_2 provide an additional mechanism to regulate Moe function at the cortex of dividing cells. Several studies have established a role of PI(4,5)P_2 in the localization of ERM proteins in polarized processes of differentiated cells (Fievet et al., 2004; Hao et al., 2009; Roch et al., 2010). Here, we provide evidence that during mitosis, PI(4,5)P_2-rich membrane domains act as a spatial cue that regulates both Moe distribution and activation at the cortex.

The distribution of PI(4,5)P_2 at the plasma membrane is tightly regulated during mitosis. As in mammalian cells (Emoto et al., 2005; Field et al., 2005), we find that PI(4,5)P_2 is actively enriched at the equator of anaphase *Drosophila* S2 cells, suggesting that equatorial accumulation of PI(4,5)P_2 is a feature shared by most animal cells. Although a previous study did not detect

PI(4,5)P$_2$ enrichment at the cleavage furrow of *Drosophila* spermatocytes (Wong et al., 2005), whether this is caused by an intrinsic difference between mitosis and meiosis or by experimental limitations in vivo remains to be established. However, how this dynamic localization is regulated remained unknown. Here, we show that the equatorial enrichment of PI(4,5)P$_2$ relies, at least in part, on the enzymatic activity of Skittles and Pten. During cytokinesis, the equatorial accumulation of PI(4,5)P$_2$ plays a role in cleavage furrow formation and ingression, through controlling the activity and/or recruitment of several components of the contractile ring (Janetopoulos and Devreotes, 2006; Ben El Kadhi et al., 2011). PI(4,5)P$_2$ hydrolysis is also necessary for maintaining cleavage furrow stability and efficient cytokinesis (Emoto et al., 2005; Field et al., 2005; Wong et al., 2005). Our findings extend the functional repertoire of PI(4,5)P$_2$ during mitosis to the control of local properties of the mitotic cortex, which are required for polar relaxation and cell elongation. Through functional screenings, we identify novel regulators of cell division among the entire set of enzymes implicated in phosphoinositide biosynthesis. Two main pathways regulate PI(4,5)P$_2$ levels in mitotic cells, and their alterations provoke similar cortical disorganization. The first pathway involves the Pten tumor suppressor, a PI(3,4,5)P$_3$ 3-phosphatase. Pten was shown to accumulate at the septum of dividing yeast cells (Mitra et al., 2004), as well as at the cleavage furrow in *Dictyostelium discoideum* (Janetopoulos et al., 2005). Our results of living *Drosophila* cells show a progressive delocalization of Pten from the polar cortex to the equator after anaphase onset (Fig. 7 B), suggesting that Pten dynamics rely on mechanisms conserved throughout evolution. Furthermore, depletion of Pten leads to a significant enrichment of PI(3,4,5)P$_3$ at the cortex, especially at the cleavage furrow. These results show that Pten uses PI(3,4,5)P$_3$ to spatially control PI(4,5)P$_2$ levels at the mitotic cortex.

The second pathway relies on Skittles, a PI(4)P 5-kinase that plays a major role in regulating the levels and localization of PI(4,5)P$_2$ during mitosis. Skittles switches from an isotropic cortical distribution in pro/metaphase to equatorial enrichment after the anaphase onset (Fig. 7 B). Depletion of Skittles results in a phenotype similar to the mitotic cortical defects observed after inducible PI(4,5)P$_2$ hydrolysis. We also find that CG10260, a phosphoinositide 4-kinase, contributes to the organization of the mitotic cortex. Genetics screens have identified a role for phosphoinositide 4-kinases in the division of budding and fission yeast (Audhya et al., 2000; Hama et al., 2000; Desautels et al., 2001) as well as for cytokinesis of male spermatocytes in flies (Brill et al., 2000). CG10260 is involved in PI(4)P synthesis, the major substrate of Skittles to produce PI(4,5)P$_2$. Together, these data show that Skittles acts as a key regulator of PI(4,5)P$_2$ levels and Moe activation at the mitotic cortex. Interestingly, Skittles is required for Moe activation in *Drosophila* oocytes (Gervais et al., 2008), suggesting that this enzyme plays a broad role in the regulation of ERM proteins.

An important question is how Skittles and Pten are enriched at the equator in anaphase. It has been reported that activated RhoA stimulates a PI(4)P 5-kinase activity and promotes PI(4,5)P$_2$ synthesis in mammalian cells (Chong et al., 1994).

During anaphase, activated RhoA localizes at the equatorial cortex (Yoshida et al., 2009), where it could recruit and/or activates Skittles to promote PI(4,5)P$_2$ production. This anisotropy in PI(4,5)P$_2$ distribution might be in turn reinforced by the localized activity of Pten, whose membrane association is itself dependent on PI(4,5)P$_2$ (unpublished data; Campbell et al., 2003; Rahdar et al., 2009). Together, the activity of Skittles and Pten could therefore provide a feed-forward regulatory loop of local PI(4,5)P$_2$ levels at the cortex of dividing cells.

Spatiotemporal regulation of Moe contributes to mitotic cell elongation

The metaphase/anaphase transition is characterized by a break in cortical symmetry, with concomitant relaxation of the polar cortex and contraction of the equator. We find that the anisotropic distribution of Moe participates in coordinating this differential in cortical tension. Overactivation of Moe impairs cell elongation and causes cytokinesis failure, suggesting that the polar cortex is too rigid for cell division. Accumulation of F-actin at the cleavage furrow can be attributed, at least in part, to a cortical flow of F-actin filaments from polar regions to the equator (Chen et al., 2008). Overactivation of Moe at the poles could block this actin cortical flow, through an excessive bridging of the actin cytoskeleton with the plasma membrane, leading to an abnormal stiffness of the polar cortex. Therefore, redistribution of activated Moe from the polar cortex to the equator participates in polar relaxation, anaphase cell elongation, and cytokinesis fidelity.

Contraction of the equatorial actomyosin ring increases the cytoplasmic pressure exerted on the plasma membrane. Relaxation of the polar cortex is thus required to dissipate this extra pressure by increasing the cellular volume, a process that was proposed to involve short-lived polar blebs (Prothero and Spencer, 1968; Brugués et al., 2010; Sedzinski et al., 2011). These polar blebs were recently found to play important roles during cell division. Perturbation of their dynamics triggers anaphase spindle rocking (Rankin and Wordeman, 2010) and destabilization of cleavage furrow positioning (Sedzinski et al., 2011). Although recent studies have addressed how cortical blebs are regulated in interphase (Charras et al., 2005, 2006), our understanding of the signalization that controls dynamics of cortical blebs in mitosis has poorly progressed since pioneering studies. Our results show that a transient recruitment of Moe at the mitotic bleb membrane is required for efficient polar bleb retraction, as are the functions of the Moe positive regulators Slik, Skittles, and Pten. Active Moe contributes to cortical bleb organization because alteration of Moe function (or regulation) disrupts actin organization and efficient bleb retraction. This leads to disorganization of the mitotic cortex, characterized by giant blebs that continue growing in an unregulated manner. Therefore, although a global decrease in Moe activity at the polar cortex contributes to cell elongation and cytokinesis, transient and local association of Moe at the rim of polar blebs is important for their retraction. If the binding of Moe to PI(4,5)P$_2$ is required at both the equator and bleb membrane, the influence of the Slik kinase on Moe activation appears different between these two regions of the anaphase cortex. Although Slik depletion abolishes

Moe recruitment to polar blebs, remnants of cortical Moe are still visible at the equator, likely as a result of high $PI(4,5)P_2$ levels at the furrow.

Although these mechanisms synergistically contribute to the cortical contractility at the equator, they also allow cortical relaxation at the polar cortex through control of transient anaphase blebs. We propose that this dual mechanism of Moe regulation is exploited by animal cells to ensure proper cell division.

Materials and methods

DNA constructs
Pten cDNA obtained from V. Archambault (Institute for Research in Immunology and Cancer, Montréal, Québec, Canada; IP16020; Drosophila Genomics Resource Center) was amplified by PCR (Phusion; New England Biolabs, Inc.) and fused to GFP in the pAc5.1 vector (Invitrogen). RCs (PM-FRB-monomeric RFP [mRFP] and mRFP-FKBP-5-phosphatase domain) obtained from T. Balla (National Institutes of Heath, Bethesda, MD; Varnai et al., 2006) and GFP-Utrophin-CH obtained from W.M. Bement (University of Wisconsin, Madison, WI; Burkel et al., 2007) were subcloned in the pAc5.1 vector (Invitrogen). pUAS-Skittles-GFP was obtained from A. Guichet (Institut Jacques Monod, Unité Mixte de Recherche 7592, Paris, France; Gervais et al., 2008), pUAS-Slik-GFP was obtained from D. Hipfner (Institut de Recherches Cliniques de Montréal, Montréal, Québec, Canada; Hipfner et al., 2004), and pUAS-GFP-Tubby and pTubulin-Grp1-PH-GFP were obtained from A.A. Kiger (University of California, San Diego, San Diego, CA). Other DNA constructs were previously described in Carreno et al. (2008).

dsRNA primers
dsRNA primers used in this study were as follows: Skittles_1 forward, 5′-TAATACGACTCACTATAGGGAGAACTGATGAGCACCATTAAGCG-3′, and reverse, 5′-TAATACGACTCACTATAGGGAGAGAATGTTTCAGTGGAA-ATGTGG-3′; Skittles_2 forward, 5′-TAATACGACTCACTATAGGGAGACC-CCCTCCAAGCGCAAAACCTCG-3′, and reverse, 5′-TAATACGACTCACT-ATAGGGAGAGCGTGGACGTGTAGCTGGGCG-3′; Pten forward, 5′-TAA-TACGACTCACTATAGGGAGACAAACGCAAACAGCCTAATAGC-3′, and reverse, 5′-TAATACGACTCACTATAGGGAGACCACAGTTGAATTTTGGAG-AGG-3′; Pten_1 forward, 5′-TAATACGACTCACTATAGGGAGATATCCA-GCACCGGATAAACTA-3′, and reverse, 5′-TAATACGACTCACTATAGGG-AGACAAGGTTTTCAGTCTATCTGG-3′; Pten_2 forward, 5′-TAATAC-GACTCACTATAGGGAGACATCAAATACCAGTTTCCGGCG-3′, and reverse, 5′-TAATACGACTCACTATAGGGAGATCGAAGTATTTTTTGAA-TTGG-3′; CG10260_1 forward, 5′-TAATACGACTCACTATAGGGAGAC-GATTCGGTGAACGAGCTGCG-3′, and reverse, 5′-TAATACGACTCACTA-TAGGGAGATCGGCGAAGTCCTTCAAGCGC-3′; CG10260_2 forward, 5′-TAATACGACTCACTATAGGGAGAGGTCTGTCGCTGCTGCAGGGC-3′, and reverse, 5′-TAATACGACTCACTATAGGGAGACCCGGCACTATAA-GATCCGGC-3′; Pp1-87B forward, 5′-TAATACGACTCACTATAGGGAGA-GATCGGAAATTAAAGATTTCGAGG-3′, and reverse, 5′-TAATACGACTC-ACTATAGGGAGAAAAGATCTTCTCGTCGACAATGG-3′; Pp1-87B 5′UTR forward, 5′-TAATACGACTCACTATAGGGAGACGGCAGTGTGGCAAC-ATCAGCTAGAAGC-3′, and reverse, 5′-TAATACGACTCACTATAGGG-AGAGTTTGCGTGCGAAAGTGTGGATCTGG-3′; Pp1-87B 3′UTR forward, 5′-TAATACGACTCACTATAGGGAGATATCACACAACTGCAGCACCACG-3′, and reverse, 5′-TAATACGACTCACTATAGGGAGACTTGCTCTATACTCTTAA-GGCC-3′; CG10260 forward, 5′-TAATACGACTCACTATAGGGAGAGGA-GTATCCCAATCAGATTCCC-3′, and reverse, 5′-TAATACGACTCACTATAGG-GAGAATCAGTATGGGCTTGCTGACC-3′; and Slik forward, 5′-TAATACGAC-TCACTATAGGGAGAACTTTGTCAAAAAGGGTAAGGC-3′, and reverse, 5′-TAATACGACTCACTATAGGGAGAACCTCACTTTCATCCAGTTTGC-3′.

Cell lines and culture
S2 Drosophila cells were cultured under standard conditions. We generated stable cell lines expressing wild-type Moe-GFP, Moe-TA-GFP, Moe-TD-GFP, FERM^{Moe}-GFP, Moe-KN-GFP, GFP-Utrophin-CH, GFP-Tubby, and Grp1-PH-GFP in combination with Tubulin-mCherry to identify mitotic stages. We used FACS sorting (FACSAria; BD) to select cell lines expressing moderate levels of the different GFP fusions. The distribution of Pp1-87B–GFP, Skittles-GFP, Pten-GFP, and Slik-GFP was analyzed after transient transfection (FuGENE HD; Roche) of the corresponding constructs. Cells stably expressing Moe-GFP or GFP-Tubby were transfected by the RC constructs 36 h before rapamycin addition (final concentration of 100 nM).

dsRNA-mediated screenings
Phosphatase subunits and phosphoinositide enzymes were identified by annotation of the fly genome complemented by a search for individual orthologues of mammalian counterparts. Production of dsRNA was previously described in Carreno et al. (2008). dsRNA were synthesized using DNA templates from the Drosophila dsRNA library (Thermo Fisher Scientific). Each positive hit was confirmed by the use of at least one additional dsRNA, targeting an independent region of the gene of interest to avoid off targets.

Immunofluorescence and video microscopy
Cells were cultured for 4 h on glass coverslips, fixed in 4% formaldehyde (or 10% TCA for P-Moe), and processed for immunostaining (Carreno et al., 2008). We used anti–P-Moe (Carreno et al., 2008) at 1:100, anti–α-tubulin coupled to FITC (F2168; Sigma-Aldrich) at 1:50, and Texas red goat anti–rabbit (Invitrogen) at 1:200. Texas red phalloidin (Invitrogen) was used at 1:100 for F-actin staining. Fixed imaging was performed at room temperature using mounting medium (Vectashield; Vector Laboratories) on a microscope (DeltaVision; Applied Precision) using softWoRx software (Applied Precision) equipped with a camera (CoolSNAP HQ2; Photometrics) at 1 × 1 binning and 60× Plan Apochromat (1.42 NA) objective.

For live imaging, cell lines were cultivated in glass-bottom plates and multichannel images were acquired at 27°C with a microscope (DeltaVision) using softWoRx software equipped with a camera (CoolSNAP HQ2) at 2 × 2 binning and 60× Plan Apochromat (1.42 NA) objective or a wide-field microscope (DMIRE2; Leica) using Metamorph software (Molecular Devices) equipped with a camera (CoolSNAP HQ2) at 2 × 2 binning and 63× Plan Apochromat (1.32 NA). Images were acquired every 15 or 7 min for broad analyses of cell division and every 7 or 20 s for fast tracking of bleb dynamics. Images were analyzed using Metamorph, softWoRx Explorer, and ImageJ (National Institutes of Health) packages. Images were deconvoluted using Scientific Volume Imaging or softWoRx and processed with Photoshop (Adobe).

Dosage of phosphoinositides
S2 cells labeled with [^{32}P]phosphate were processed for lipid extraction and separation by TLC using $CHCl_3/CH_3COCH_3/CH_3OH/CH_3COOH/H_2O$ (80:30:26:24:14 vol/vol) as a solvent. The TLC plate (silica gel 60 with concentrating zone; Merck) had been treated with 1% potassium-oxalate in 2 mM EDTA/methanol (vol/vol) for 15 min and activated at 100°C for 1 h. Spots corresponding to phosphoinositol phosphate and $PI(4,5)P_2$ were visualized with a PhosphoImager scanner (GE Healthcare), identified by comparison with the migration of authentic standards, scraped off separately, and deacylated by adding 1 ml methylamine reagent composed of 26.8% (vol/vol) of 40% methylamine, 45.7% (vol/vol) methanol, 11.4% (vol/vol) n-butanol, and 16% (vol/vol) H_2O to the silica powder. After incubation at 53°C for 50 min, the methylamine reagent was completely evaporated under a nitrogen stream at 37°C. The samples were resuspended in 1.2 ml H_2O and separated by HPLC using a column (Partisphere 5 SAX; Whatman) 4.6 × 125 mm with guard cartridge anion exchanger units (Whatman) and a gradient of 1 M $(NH_4)2HPO_4$, pH 3.8, and bidistilled water as previously described (Payrastre, 2004).

SDS-PAGE and P-Moe Western blotting
For each condition (controls, dsRNA, or 50 nM Calyculin A–treated cells), 10^6 cells were washed with 1 ml PBS $NaF/Na_3VO_4/β$-glycerophosphate (50 mM/1 mM/40 mM). After centrifugation (5 min at 4°C), pellets were resuspended in 100 µl Laemmli buffer at 95°C supplemented with antiphosphatases and antiprotease cocktail (Roche). Membranes were blocked with TBS Tween/BSA/NaF/$Na_3VO_4/β$-glycerophosphate (0.1%/2%/50 mM/5 mM/40 mM) and then incubated with an antibody against Moe (1:25,000) or P-Moe (1:200).

Flow cytometry
Cells were fixed for 4 h using ethanol 75% and permeabilized by 0.02% saponin. Cells were labeled using anti–P-Moe (1:100), antiphospho–histone H3 (Ser10) 647 conjugate (1:100; Cell Signaling Technology), and Alexa Fluor 488 goat anti–rabbit (1:1,000; Invitrogen) antibodies. Cells were then analyzed by FACS (LSR II; BD).

Online supplemental material
Fig. S1 shows localization of sqh-GFP during mitotic blebbing and quantification of mitotic bleb dynamics in control and Slik dsRNA conditions. Fig. S2 shows characterization of Pp1-87B function during cell division. Fig. S3 shows localization of Moe-TA-GFP during cell division. Fig. S4 shows quantification

of the RC experiments shown in Fig. 4. Fig. S5 shows the results of the functional screen for enzymes implicated in phosphoinositide metabolism shown in Fig. 5. Video 1 shows the dynamic localization of Moe-GFP during division of a control cell over a 25-min period with a 1-min interval (as shown in Fig. 1 B). Video 2 shows the dynamic localization of Moe-GFP during division of a control cell over a 675-s period with a 7-s interval (as shown in Fig. 2 A). Video 3 shows the dynamic localization of Moe-GFP during division of a Slik-depleted cell over a 500-s period with a 20-s interval (as shown in Fig. 2 A). Video 4 shows the dynamic localization of Utrophin-CH-GFP (as an F-actin probe) during division of a control cell over a 337.5-s period with a 2.5-s interval (as shown in Fig. 2 C). Video 5 shows the dynamic localization of Utrophin-CH-GFP (as an F-actin probe) during division of a Slik-depleted cell over a 225-s period with a 2.5-s interval (as shown in Fig. 2 C). Video 6 shows the dynamic localization of GFP-Tubby (as a PI(4,5)P$_2$ probe) in interphase RC cells before and after addition of rapamycin over a 450-s period with a 15-s interval (as shown in Fig. 4 E). Video 7 shows the dynamic localization of Moe-GFP of a metaphase RC cell before and after addition of rapamycin over a 300-s period with a 10-s interval (as shown in Fig. 4 E). Video 8 shows the dynamic localization of Moe-GFP of an ana/telophase RC cell 435 s after addition of rapamycin over a 603-s period with a 9-s interval (as shown in Fig. 4 F). Video 9 shows the dynamic localization of Moe-GFP during division of a Skittles-depleted cell over a 90-min period with a 10-min interval (as shown in Fig. 6 D). Video 10 shows the dynamic localization of Utrophin-CH-GFP (as an F-actin probe) during division of a Skittles-depleted cell over a 217.5-s period with a 7.5-s interval (as shown in Fig. 6 E). Online supplemental material is available at http://www.jcb.org/cgi/content/full/jcb.201106048/DC1.

References

Audhya, A., M. Foti, and S.D. Emr. 2000. Distinct roles for the yeast phosphatidylinositol 4-kinases, Stt4p and Pik1p, in secretion, cell growth, and organelle membrane dynamics. *Mol. Biol. Cell.* 11:2673–2689.

Axton, J.M., V. Dombrádi, P.T. Cohen, and D.M. Glover. 1990. One of the protein phosphatase 1 isoenzymes in *Drosophila* is essential for mitosis. *Cell.* 63:33–46. http://dx.doi.org/10.1016/0092-8674(90)90286-N

Ben El Kadhi, K., C. Roubinet, S. Solinet, G. Emery, and S. Carréno. 2011. The inositol 5-phosphatase dOCRL controls PI(4,5)P2 homeostasis and is necessary for cytokinesis. *Curr. Biol.* 21:1074–1079. http://dx.doi .org/10.1016/j.cub.2011.05.030

Boucrot, E., and T. Kirchhausen. 2007. Endosomal recycling controls plasma membrane area during mitosis. *Proc. Natl. Acad. Sci. USA.* 104:7939–7944. http://dx.doi.org/10.1073/pnas.0702511104

Brill, J.A., G.R. Hime, M. Scharer-Schuksz, and M.T. Fuller. 2000. A phospholipid kinase regulates actin organization and intercellular bridge formation during germline cytokinesis. *Development.* 127:3855–3864.

Brugués, J., B. Maugis, J. Casademunt, P. Nassoy, F. Amblard, and P. Sens. 2010. Dynamical organization of the cytoskeletal cortex probed by micropipette aspiration. *Proc. Natl. Acad. Sci. USA.* 107:15415–15420. http://dx.doi .org/10.1073/pnas.0913669107

Burkel, B.M., G. von Dassow, and W.M. Bement. 2007. Versatile fluorescent probes for actin filaments based on the actin-binding domain of utrophin. *Cell Motil. Cytoskeleton.* 64:822–832. http://dx.doi.org/10.1002/ cm.20226

Burton, K., and D.L. Taylor. 1997. Traction forces of cytokinesis measured with optically modified elastic substrata. *Nature.* 385:450–454. http://dx.doi .org/10.1038/385450a0

Campbell, R.B., F. Liu, and A.H. Ross. 2003. Allosteric activation of PTEN phosphatase by phosphatidylinositol 4,5-bisphosphate. *J. Biol. Chem.* 278:33617–33620. http://dx.doi.org/10.1074/jbc.C300296200

Carreno, S., I. Kouranti, E.S. Glusman, M.T. Fuller, A. Echard, and F. Payre. 2008. Moesin and its activating kinase Slik are required for cortical stability and microtubule organization in mitotic cells. *J. Cell Biol.* 180:739–746. http://dx.doi.org/10.1083/jcb.200709161

Charras, G.T., J.C. Yarrow, M.A. Horton, L. Mahadevan, and T.J. Mitchison. 2005. Non-equilibration of hydrostatic pressure in blebbing cells. *Nature.* 435:365–369. http://dx.doi.org/10.1038/nature03550

Charras, G.T., C.K. Hu, M. Coughlin, and T.J. Mitchison. 2006. Reassembly of contractile actin cortex in cell blebs. *J. Cell Biol.* 175:477–490. http:// dx.doi.org/10.1083/jcb.200602085

Chen, F., V. Archambault, A. Kar, P. Lio', P.P. D'Avino, R. Sinka, K. Lilley, E.D. Laue, P. Deak, L. Capalbo, and D.M. Glover. 2007. Multiple protein phosphatases are required for mitosis in *Drosophila. Curr. Biol.* 17:293–303. http://dx.doi.org/10.1016/j.cub.2007.01.068

Chen, W., M. Foss, K.F. Tseng, and D. Zhang. 2008. Redundant mechanisms recruit actin into the contractile ring in silkworm spermatocytes. *PLoS Biol.* 6:e209. http://dx.doi.org/10.1371/journal.pbio.0060209

Cheng, J., A. Tiyaboonchai, Y.M. Yamashita, and A.J. Hunt. 2011. Asymmetric division of cyst stem cells in *Drosophila* testis is ensured by anaphase spindle repositioning. *Development.* 138:831–837. http://dx.doi .org/10.1242/dev.057901

Chong, L.D., A. Traynor-Kaplan, G.M. Bokoch, and M.A. Schwartz. 1994. The small GTP-binding protein Rho regulates a phosphatidylinositol 4-phosphate 5-kinase in mammalian cells. *Cell.* 79:507–513. http://dx.doi .org/10.1016/0092-8674(94)90259-3

Coscoy, S., F. Waharte, A. Gautreau, M. Martin, D. Louvard, P. Mangeat, M. Arpin, and F. Amblard. 2002. Molecular analysis of microscopic ezrin dynamics by two-photon FRAP. *Proc. Natl. Acad. Sci. USA.* 99:12813–12818. http://dx.doi.org/10.1073/pnas.192084599

Desautels, M., J.P. Den Haese, C.M. Slupsky, L.P. McIntosh, and S.M. Hemmingsen. 2001. Cdc4p, a contractile ring protein essential for cytokinesis in *Schizosaccharomyces pombe*, interacts with a phosphatidylinositol 4-kinase. *J. Biol. Chem.* 276:5932–5942. http://dx.doi .org/10.1074/jbc.M008715200

De Wulf, P., F. Montani, and R. Visintin. 2009. Protein phosphatases take the mitotic stage. *Curr. Opin. Cell Biol.* 21:806–815. http://dx.doi.org/ 10.1016/j.ceb.2009.08.003

Emoto, K., H. Inadome, Y. Kanaho, S. Narumiya, and M. Umeda. 2005. Local change in phospholipid composition at the cleavage furrow is essential for completion of cytokinesis. *J. Biol. Chem.* 280:37901–37907. http:// dx.doi.org/10.1074/jbc.M504282200

Fehon, R.G., A.I. McClatchey, and A. Bretscher. 2010. Organizing the cell cortex: the role of ERM proteins. *Nat. Rev. Mol. Cell Biol.* 11:276–287. http://dx.doi.org/10.1038/nrm2866

Field, S.J., N. Madson, M.L. Kerr, K.A. Galbraith, C.E. Kennedy, M. Tahiliani, A. Wilkins, and L.C. Cantley. 2005. PtdIns(4,5)P2 functions at the cleavage furrow during cytokinesis. *Curr. Biol.* 15:1407–1412. http://dx.doi .org/10.1016/j.cub.2005.06.059

Fievet, B.T., A. Gautreau, C. Roy, L. Del Maestro, P. Mangeat, D. Louvard, and M. Arpin. 2004. Phosphoinositide binding and phosphorylation act sequentially in the activation mechanism of ezrin. *J. Cell Biol.* 164:653–659. http://dx.doi.org/10.1083/jcb.200307032

Fishkind, D.J., L.G. Cao, and Y.L. Wang. 1991. Microinjection of the catalytic fragment of myosin light chain kinase into dividing cells: effects on mitosis and cytokinesis. *J. Cell Biol.* 114:967–975. http://dx.doi .org/10.1083/jcb.114.5.967

Flemming, W. 1882. Zellsubstanz, Kern und Zelltheilung. F.C.W. Vogel, Leipzig, Germany. 478 pp.

Gervais, L., S. Claret, J. Januschke, S. Roth, and A. Guichet. 2008. PIP5K-dependent production of PIP2 sustains microtubule organization to establish polarized transport in the *Drosophila* oocyte. *Development.* 135:3829–3838. http://dx.doi.org/10.1242/dev.029009

Gray, A., J. Van Der Kaay, and C.P. Downes. 1999. The pleckstrin homology domains of protein kinase B and GRP1 (general receptor for

phosphoinositides-1) are sensitive and selective probes for the cellular detection of phosphatidylinositol 3,4-bisphosphate and/or phosphatidylinositol 3,4,5-trisphosphate in vivo. *Biochem. J.* 344:929–936. http://dx.doi.org/10.1042/0264-6021:3440929

Hama, H., J.Y. Takemoto, and D.B. DeWald. 2000. Analysis of phosphoinositides in protein trafficking. *Methods*. 20:465–473. http://dx.doi.org/10.1006/meth.2000.0959

Hao, J.J., Y. Liu, M. Kruhlak, K.E. Debell, B.L. Rellahan, and S. Shaw. 2009. Phospholipase C–mediated hydrolysis of PIP2 releases ERM proteins from lymphocyte membrane. *J. Cell Biol.* 184:451–462. http://dx.doi.org/10.1083/jcb.200807047

Hickson, G.R., A. Echard, and P.H. O'Farrell. 2006. Rho-kinase controls cell shape changes during cytokinesis. *Curr. Biol.* 16:359–370. http://dx.doi.org/10.1016/j.cub.2005.12.043

Hipfner, D.R., N. Keller, and S.M. Cohen. 2004. Slik Sterile-20 kinase regulates Moesin activity to promote epithelial integrity during tissue growth. *Genes Dev.* 18:2243–2248. http://dx.doi.org/10.1101/gad.303304

Janetopoulos, C., and P. Devreotes. 2006. Phosphoinositide signaling plays a key role in cytokinesis. *J. Cell Biol.* 174:485–490. http://dx.doi.org/10.1083/jcb.200603156

Janetopoulos, C., J. Borleis, F. Vazquez, M. Iijima, and P. Devreotes. 2005. Temporal and spatial regulation of phosphoinositide signaling mediates cytokinesis. *Dev. Cell.* 8:467–477. http://dx.doi.org/10.1016/j.devcel.2005.02.010

Kunda, P., A.E. Pelling, T. Liu, and B. Baum. 2008. Moesin controls cortical rigidity, cell rounding, and spindle morphogenesis during mitosis. *Curr. Biol.* 18:91–101. http://dx.doi.org/10.1016/j.cub.2007.12.051

Luxenburg, C., H.A. Pasolli, S.E. Williams, and E. Fuchs. 2011. Developmental roles for Srf, cortical cytoskeleton and cell shape in epidermal spindle orientation. *Nat. Cell Biol.* 13:203–214. http://dx.doi.org/10.1038/ncb2163

Maddox, A.S., and K. Burridge. 2003. RhoA is required for cortical retraction and rigidity during mitotic cell rounding. *J. Cell Biol.* 160:255–265. http://dx.doi.org/10.1083/jcb.200207130

Matzke, R., K. Jacobson, and M. Radmacher. 2001. Direct, high-resolution measurement of furrow stiffening during division of adherent cells. *Nat. Cell Biol.* 3:607–610. http://dx.doi.org/10.1038/35078583

Mitra, P., Y. Zhang, L.E. Rameh, M.P. Ivshina, D. McCollum, J.J. Nunnari, G.M. Hendricks, M.L. Kerr, S.J. Field, L.C. Cantley, and A.H. Ross. 2004. A novel phosphatidylinositol(3,4,5)P$_3$ pathway in fission yeast. *J. Cell Biol.* 166:205–211. http://dx.doi.org/10.1083/jcb.200404150

Payrastre, B. 2004. Phosphoinositides: lipid kinases and phosphatases. *Methods Mol. Biol.* 273:201–212.

Porter, K., D. Prescott, and J. Frye. 1973. Changes in surface morphology of Chinese hamster ovary cells during the cell cycle. *J. Cell Biol.* 57:815–836. http://dx.doi.org/10.1083/jcb.57.3.815

Prothero, J.W., and D. Spencer. 1968. A model of blebbing in mitotic tissue culture cells. *Biophys. J.* 8:41–51. http://dx.doi.org/10.1016/S0006-3495(68)86473-2

Rahdar, M., T. Inoue, T. Meyer, J. Zhang, F. Vazquez, and P.N. Devreotes. 2009. A phosphorylation-dependent intramolecular interaction regulates the membrane association and activity of the tumor suppressor PTEN. *Proc. Natl. Acad. Sci. USA*. 106:480–485. http://dx.doi.org/10.1073/pnas.0811212106

Rankin, K.E., and L. Wordeman. 2010. Long astral microtubules uncouple mitotic spindles from the cytokinetic furrow. *J. Cell Biol.* 190:35–43. http://dx.doi.org/10.1083/jcb.201004017

Rappaport, R. 1971. Cytokinesis in animal cells. *Int. Rev. Cytol.* 31:169–213. http://dx.doi.org/10.1016/S0074-7696(08)60059-5

Roch, F., C. Polesello, C. Roubinet, M. Martin, C. Roy, P. Valenti, S. Carreno, P. Mangeat, and F. Payre. 2010. Differential roles of PtdIns(4,5)P2 and phosphorylation in moesin activation during *Drosophila* development. *J. Cell Sci.* 123:2058–2067. http://dx.doi.org/10.1242/jcs.064550

Rogers, S.L., U. Wiedemann, U. Häcker, C. Turck, and R.D. Vale. 2004. *Drosophila* RhoGEF2 associates with microtubule plus ends in an EB1-dependent manner. *Curr. Biol.* 14:1827–1833. http://dx.doi.org/10.1016/j.cub.2004.09.078

Sedzinski, J., M. Biro, A. Oswald, J.Y. Tinevez, G. Salbreux, and E. Paluch. 2011. Polar actomyosin contractility destabilizes the position of the cytokinetic furrow. *Nature*. 476:462–466. http://dx.doi.org/10.1038/nature10286

Stewart, M.P., J. Helenius, Y. Toyoda, S.P. Ramanathan, D.J. Muller, and A.A. Hyman. 2011. Hydrostatic pressure and the actomyosin cortex drive mitotic cell rounding. *Nature*. 469:226–230. http://dx.doi.org/10.1038/nature09642

Surcel, A., Y.S. Kee, T. Luo, and D.N. Robinson. 2010. Cytokinesis through biochemical-mechanical feedback loops. *Semin. Cell Dev. Biol.* 21:866–873. http://dx.doi.org/10.1016/j.semcdb.2010.08.003

Szentpetery, Z., A. Balla, Y.J. Kim, M.A. Lemmon, and T. Balla. 2009. Live cell imaging with protein domains capable of recognizing phosphatidylinositol 4,5-bisphosphate; a comparative study. *BMC Cell Biol.* 10:67. http://dx.doi.org/10.1186/1471-2121-10-67

Théry, M., and M. Bornens. 2008. Get round and stiff for mitosis. *HFSP J.* 2:65–71. http://dx.doi.org/10.2976/1.2895661

Trinkle-Mulcahy, L., J. Andersen, Y.W. Lam, G. Moorhead, M. Mann, and A.I. Lamond. 2006. Repo-Man recruits PP1γ to chromatin and is essential for cell viability. *J. Cell Biol.* 172:679–692. http://dx.doi.org/10.1083/jcb.200508154

Varnai, P., B. Thyagarajan, T. Rohacs, and T. Balla. 2006. Rapidly inducible changes in phosphatidylinositol 4,5-bisphosphate levels influence multiple regulatory functions of the lipid in intact living cells. *J. Cell Biol.* 175:377–382. http://dx.doi.org/10.1083/jcb.200607116

Wong, R., I. Hadjiyanni, H.C. Wei, G. Polevoy, R. McBride, K.P. Sem, and J.A. Brill. 2005. PIP2 hydrolysis and calcium release are required for cytokinesis in *Drosophila* spermatocytes. *Curr. Biol.* 15:1401–1406. http://dx.doi.org/10.1016/j.cub.2005.06.060

Yoshida, S., S. Bartolini, and D. Pellman. 2009. Mechanisms for concentrating Rho1 during cytokinesis. *Genes Dev.* 23:810–823. http://dx.doi.org/10.1101/gad.1785209